THE JOURNAL OF BIOLOGICAL CHEMISTRY
Vol. 280, No. 3, Issue of January 21, pp. 2092–2104, 2005
Printed in U.S.A.

Genes Affecting the Cell Cycle, Growth, Maintenance, and Drug Sensitivity Are Preferentially Regulated by Anti-HER2 Antibody through Phosphatidylinositol 3-Kinase-AKT Signaling*

Received for publication, March 19, 2004, and in revised form, October 21, 2004
Published, JBC Papers in Press, October 25, 2004, DOI 10.1074/jbc.M403080200

Xiao-Feng Le‡, Amy Lammayot‡, David Gold§, Yiling Lu¶, Weiqun Mao‡, Teresa Chang‡, Adarsh Patel‡, Gordon B. Mills¶, and Robert C. Bast, Jr.‡‖

From the Departments of ‡Experimental Therapeutics, §Biostatistics, and ¶Molecular Therapeutics, the University of Texas M. D. Anderson Cancer Center, Houston, Texas 77030

The molecular mechanisms by which the anti-HER2 antibodies trastuzumab and its murine equivalent 4D5 inhibit tumor growth and potentiate chemotherapy are not fully understood. Inhibition of signaling through the phosphatidylinositol 3-kinase (PI3K)-AKT pathway may be particularly important. Treatment of breast cancer cells that overexpress HER2 with trastuzumab inhibited HER2-HER3 association, decreased PDK1 activity, reduced Thr-308 and Ser-473 phosphorylation of AKT, and reduced AKT enzymatic activity. To place the role of PI3K-AKT in perspective, gene expression was studied by using Affymetrix microarrays and real time reverse transcription-PCR. Sixteen genes were consistently down-regulated 2.0–4.9-fold in two antibody-treated breast cancer cell lines. Fourteen of the 16 genes were involved in three major functional areas as follows: 7 in cell cycle regulation, particularly of the G_2-M; 5 in DNA repair/replication; and 2 in modifying chromatin structure. Of the 16 antibody-regulated genes, 64% had roles in cell growth/maintenance and 52% contributed to the cell cycle. Direct inhibition of PI3K with an inhibitor markedly reduced expression of 14 genes that were also affected by the antibody. Constitutive activation of AKT1 blocked the effect of the anti-HER2 antibody on cell cycle arrest and on eight differentially expressed genes. The antibody enhanced docetaxel-induced growth inhibition but did not increase the fraction of apoptotic cells induced with docetaxel alone. In contrast, the antibody plus docetaxel markedly down-regulated two genes, *HEC* and *DEEPEST*, required for passage through G_2-M. Thus, anti-HER2 antibody preferentially affects genes contributing to cell cycle progression and cell growth/maintenance, in part through the PI3K-AKT signaling. Transcriptional regulation by anti-HER2 antibody through PI3K-AKT pathway may potentiate the growth inhibitory activity of docetaxel by affecting cell cycle progression.

The human epidermal growth factor receptor 2 (HER2,[1] also known as c-Neu or ErbB-2) encodes a 185-kDa transmembrane tyrosine kinase growth factor receptor. The ligand that binds to the homodimers of HER2 has not yet been identified. Rather, HER2 functions as a preferred co-receptor to form heterodimers with HER1 (epidermal growth factor receptor), HER3, or HER4. Of these heterodimers, HER2-HER3 is particularly important for intracellular signaling (1). HER2 signaling has been linked to a variety of cellular responses to growth factors under both normal and pathophysiological conditions. HER2 signaling is required not only during normal development of the mammary gland but also during development of the glia, neurons, and heart (1, 2). Amplification of the *HER2* gene and overexpression of HER2 protein have been documented in ~30% of breast and 15% of ovarian cancers (3). In many (but not all) reports, HER2 overexpression has been associated with a more aggressive course of disease. Although the underlying mechanisms for this association are still not well characterized, HER2 overexpression has been linked to increased proliferation and invasiveness (4).

HER2 is currently one of the best defined targets for specific therapy. The substantially greater expression of HER2 on cancer cells than on normal epithelial tissues permits selective targeting of malignant cells. HER2 is expressed on the cell surface where it can interact with ligands and antibodies (1–4). Trastuzumab, a monoclonal antibody directed against the extracellular domain of HER2, is therapeutically active in HER2-positive breast carcinomas (3). Clinical trials in HER2-positive patients with breast cancer have demonstrated that targeted therapy with trastuzumab in conjunction with cytotoxic chemotherapy (such as platinum compounds, taxanes, and anthracyclines) improves time to disease progression and overall survival (3, 5). Clinical trials have also documented an increased risk for cardiotoxicity when trastuzumab is combined with anthracyclines, suggesting that HER2 signaling may contribute to normal heart function.

The mechanisms by which trastuzumab affects growth of HER2-positive cancer cells and enhances sensitivity to chemotherapy are not fully understood. Anti-HER2 antibody can down-regulate the HER2 receptor and prevent cleavage of the extracellular domain of the receptor (13). Receptors are, however, generally re-expressed within a matter of hours, and binding of anti-HER2 antibody can also alter intracellular signaling by enhancing kinase activity and preventing heterodimer formation. Our group and others have demonstrated that anti-HER2 monoclonal antibodies exert inhibitory effects

* This work was supported in part by NCI Grant CA39930 from the National Institutes of Health (to R. C. B.) and by Grant 80094241 from the Goodwin Foundation (to X.-F. L.). The costs of publication of this article were defrayed in part by the payment of page charges. This article must therefore be hereby marked "*advertisement*" in accordance with 18 U.S.C. Section 1734 solely to indicate this fact.

‖ To whom correspondence should be addressed: University of Texas M. D. Anderson Cancer Center, 1515 Holcombe Blvd., Box 355, Houston, TX 77030-4009. Tel.: 713-792-7743; Fax: 713-792-7864; E-mail: rbast@mdanderson.org.

[1] The abbreviations used are: HER2, human epidermal growth factor receptor 2; PI3K, phosphatidylinositol 3-kinase; RT, reverse transcription; PCNA, proliferating cell nuclear antigen; FC, fold change; GAPDH, glyceraldehyde-3-phosphate dehydrogenase; MES, 4-morpholineethanesulfonic acid; PBS, phosphate-buffered saline; hIgG, human IgG; m, mammalian.

on HER2-overexpressing breast cancer cells through induction of G_1 cell cycle arrest associated with induction of $p27^{Kip1}$ and reduction of CDK2 (6–11). We have further shown that post-translational regulation of $p27^{Kip1}$ plays a critical role in the anti-HER2 antibody-mediated G_1 cell cycle arrest and tumor growth inhibition (12). Of the post-translational mechanisms, we have shown that modulation of the phosphorylation of $p27^{Kip1}$ protein is the mechanism by which anti-HER2 antibody up-regulates the protein (12). Anti-HER2 antibodies that inhibit tumor growth also prevent HER2-HER3 interaction and inhibit the PI3K-AKT signaling pathway (6, 11, 16, 17). As the PI3K-AKT pathway is critically important to cell survival signaling, inhibition of the PI3K-AKT pathway may explain, in part, the ability of trastuzumab to enhance paclitaxel-induced apoptosis (20). Trastuzumab also suppresses DNA repair capacity (18) through as yet unknown pathways, contributing to the ability of the antibody to enhance the anti-tumor effect of DNA-damaging agents such as cisplatin (18) and radiotherapy (19). *In vivo*, trastuzumab inhibits angiogenesis and induces antibody-dependent cellular cytotoxicity (13, 14), potentially contributing to its activity. Loss or blockade of the FcγRIII receptor on leukocytes has been shown to severely impair the anti-tumor effect of trastuzumab *in vivo* (15), indicating involvement of Fc-receptor-dependent mechanisms.

Of the several mechanisms proposed for the action of anti-HER2 antibodies, interruption of the PI3K-AKT pathway may be critical for enhancing sensitivity to docetaxel and other cytotoxic drugs. Our current study explored the mechanisms of action of the anti-HER2 antibody and the impact of the antibody on activation of AKT as well as on sensitivity to docetaxel. Anti-HER2 antibody alone inhibited HER2-HER3 association, decreased PDK1 activity, reduced Thr-308 phosphorylation of AKT, and reduced AKT enzymatic activity. We have used a pharmacogenomic approach to compare the global changes that occur after treatment with anti-HER2 antibody and after treatment with the chemical inhibitor of PI3K. Treatment with anti-HER2 antibody decreased the expression of 16 genes. Fourteen of these 16 genes contribute to the following three different areas of cell function: cell cycle regulation, DNA repair/replication, and modification of chromatin structure. Direct inhibition of PI3K markedly decreased the expression of 14 genes regulated by the anti-HER2 antibody. Conversely, dominant active AKT prevented cell cycle G_1 arrest and down-regulation of cell cycle genes induced by anti-HER2 antibody. A combination of anti-HER2 antibody and docetaxel exerted additive growth inhibition against breast cancer cell lines that overexpressed HER2. The combination did not increase the fraction of apoptotic cells induced with docetaxel alone but markedly down-regulated two genes that participate in cell cycle regulation, *HEC* and *DEEPEST*, required for passage through G_2-M.

MATERIALS AND METHODS

Cell Culture—The human breast cancer cell lines, SKBr3 and BT474, were obtained from the American Type Culture Collection (ATCC, Manassas, VA). SKBr3 cells were grown in complete medium that contained RPMI 1640 (Invitrogen) supplemented with 10% fetal bovine serum (Sigma), 2 mM L-glutamine, 100 units/ml of penicillin, and 100 μg/ml streptomycin in humidified air with 5% CO_2 at 37 °C. BT474 cells were grown in complete medium containing Dulbecco's modified Eagle's medium (Invitrogen) supplemented with 10% fetal bovine serum, 2 mM L-glutamine, 1 mM sodium pyruvate (Sigma), 100 units/ml penicillin, and 100 μg/ml streptomycin. For all experiments, cells were detached with 0.25% trypsin, 0.02% EDTA. For cell culture, $2–6 \times 10^5$ exponentially growing cells were plated into 100-mm tissue culture dishes or 3×10^3 into 96-well plates in complete medium. After culture overnight in complete medium, cells were treated with anti-HER2 antibody 4D5 at 5–10 μg/ml (for SKBr3) or trastuzumab at 10 μg/ml (for BT474) in complete medium at 37 °C for 24 (for SKBr3) or 48 h (for BT474). Monoclonal antibody MOPC21 served as control antibody for 4D5 and was used at 5–10 μg/ml in SKBr3 cells. Human IgG served as control antibody for trastuzumab and was used at 10 μg/ml in BT474 cells.

Reagents—Anti-HER2 murine monoclonal antibody 4D5 and humanized monoclonal antibody trastuzumab (Herceptin®) were kindly provided by Genentech (South San Francisco, CA). MOPC21 murine myeloma cells were obtained from the American Type Culture Collection (ATCC, Manassas, VA). MOPC21 cells were grown in the peritoneal cavities of BALB/c mice to produce ascites fluid, and the immunoglobulin was purified as reported previously (25). A control IgG_1 was purchased from Calbiochem and further dialyzed against sterile cold PBS to eliminate sodium azide. Antibodies reactive with phospho-Ser-473 AKT, phospho-Thr-308 AKT, and total AKT as well as an AKT kinase assay kit were purchased from Cell Signaling Technology, Inc. (Beverly, MA). A monoclonal antibody to PCNA was purchased from BioGenex (San Ramon, CA). An antibody to AKT1 and a PDK1 kinase assay kit were obtained from Upstate Biotechnology, Inc. (Lake Placid, NY). An antibody reactive with HER2 (for Western blotting) was purchased from Oncogene Research Products (Cambridge, MA). An antibody to HER3 (for Western blotting and immunoprecipitation) was purchased from Santa Cruz Biotechnology, Inc. (Santa Cruz, CA). A monoclonal antibody to β-actin was purchased from Sigma. Recombinant human heregulin β1 (hereafter named heregulin) was obtained from NeoMarkers, Inc. (Fremont, CA). Affymetrix Human Genome U95Av2 Gene Chips that permitted measurement of the expression of 12,000 human genes were purchased from Affymetrix (Santa Clara, CA).

Preparation of Total RNA—SKBr3 cells were treated with 4D5 (10 μg/ml) or MOPC21 (10 μg/ml) for 24 h. BT474 cells were treated with trastuzumab (10 μg/ml) or hIgG (10 μg/ml) for 48 h. Total RNA was then extracted from the treated SKBr3 or BT474 cells using the TRIzol reagent (Invitrogen). Procedures were performed according to the manufacturers' recommendation. The purity of RNA was assessed by absorption at 260 and 280 nm (values of the ratio of A_{260}/A_{280} of 1.9–2.1 were considered acceptable) and by ethidium bromide staining of 18 S and 28 S RNA on gel electrophoresis. RNA concentrations were determined from the A_{260}. Only samples of intact RNA were used for subsequent Affymetrix and RT-PCR analysis.

Preparation of Fragmented cRNA for Affymetrix Analysis—A total of 15 μg of total RNA were used in the first-strand cDNA synthesis with T7-$(dT)_{24}$ primer (GGCCAGTGAATTGTAATACGACTCACTATAGGG-AGGCGG-$(dT)_{24}$) (Proligo, Boulder, CO) by Superscript II (Invitrogen). The second-strand cDNA synthesis was carried out at 16 °C by adding *Escherichia coli* DNA ligase, *E. coli* DNA polymerase I, and RNase H into the reaction. This was followed by the addition of T4 DNA polymerase to blunt the ends of newly synthesized cDNA. Double-stranded cDNA was then purified by phase lock gel (Eppendorf, Westbury, NY) with phenol/chloroform extraction. The purified cDNA was then used as templates in an *in vitro* transcription to produce cRNA labeled with biotin using the BioArray High Yield RNA transcript labeling kit from Enzo Diagnostics, Inc. (Farmingdale, NY). The procedure was carried out according to the manufacturer's recommendation, and cRNA was further purified with a Qiagen RNeasy mini kit (Valencia, CA). Approximately 15 μg of cRNA was fragmented by incubating in a buffer containing 200 mM Tris acetate (pH 8.1), 500 mM potassium acetate, and 150 mM magnesium acetate at 95 °C for 30 min. Agarose gel electrophoresis was performed before the synthesis of cRNA and after the fragmentation of cRNA to ensure the quality of the samples. Only intact, high quality cRNA samples were used for subsequent array hybridization.

Affymetrix Oligonucleotide Array Hybridization and Data Acquisition—cRNA hybridization to the human U95A arrays was performed at the M. D. Anderson Cancer Center Gene Microarray Facility by using an Affymetrix GeneChip System (Affymetrix, Santa Clara, CA). The fragmented cRNA was hybridized with pre-equilibrated Affymetrix chips at 45 °C for 16 h. Hybridized chips were then washed in a fluidic station with nonstringent buffer (6× SSPE (1× SSPE is 0.18 mol/liter NaCl, plus 0.015 mol of sodium citrate), 0.01% Tween 20, and 0.005% antifoam) for 10 cycles and with stringent buffer (100 mmol/liter MES, 0.1 mol/liter NaCl, and 0.01% Tween 20) for 4 cycles, and stained with streptavidin-phycoerythrin. This was followed by incubation with biotinylated mouse anti-avidin antibody. The chips were scanned in an Agilent ChipScanner to detect hybridization signals. Average target intensity was set at 500 arbitrary units. Each array was assessed for quality and stability by examining replicate copies of the same gene at different locations on the array. To ensure the quality of the cRNA samples and of the Affymetrix GeneChips, quality control experiments were performed using test chips, and the same cRNA sample before the test samples were processed. Further details are available from the

CCSG shared resources web site (www.mdanderson.org/departments/dnamicroarray). The raw data (hybridization data) generated by MAS 5.0 were imported into Microsoft Excel and transferred to our Department of Biostatistics for analysis.

Statistical Analysis of Affymetrix Array Data—Before analyzing the Affymetrix array data, every Affymetrix Hu95Av2 Gene Chip from our experiments underwent the following quality control checks: 1) scanner alignment and the proper dicing of images into correct cells; 2) overall chip brightness; and 3) spatial variation. Scanner alignment was checked by using the alternating pattern of positive and negative control cells on the border of each GeneChip (Affymetrix, Santa Clara, CA). The intensities of positive and negative controls were plotted as a function of border position to obtain visual confirmation that each image had been correctly aligned. Brightness was examined by looking at the histograms of detection p values (provided by Affymetrix MAS 5.0) for each array. Detection p values measure how likely a transcript was expressed at a level to be called present on the array. As a general rule, chips are flagged if less than 10% of probe sets are detected at the $p = 0.01$ level. Spatial variation is not easily detected one chip at a time, so we compared the log transformed median corrected ratio (Z) for each cell between each combination of chips A and B ($Z = \log_2(A/B) - \text{median}(\log_2(A/B))$). The range in Z was additionally constrained to enhance visual artifacts on the slide. All checks were passed for each chip.

Two array methods were used to analyze differential gene expression. A standard Affymetrix MAS 5.0 statistical analysis tool package was used for each probe set to measure fold change (FC) on the $\log_2$ scale, a 95% confidence interval for FC on the $\log_2$ scale, a p value for detection used to make the presence or absence calls for each gene, and a p value for detecting change or differential expression between samples. The default standard Affymetrix change calls were not used. Here a probe set was considered differentially expressed if the change p value was very small, the detection p value in at least one sample being compared was small, and the absolute lower bound of $\log_2$(FC), the log ratio, exceeded 0.8, corresponding to at least a 1.75-fold change. A second method designated the position-dependent nearest neighbor model was developed by Dr. Li Zhang at the Department of Biostatistics, M.D. Anderson Cancer Center (17). The position-dependent nearest neighbor model (available at the following web site: odin.mdacc.tmc.edu/~zhangli/PerfectMatch/) relies on a relationship between DNA base pair stacking energies and probe binding efficiencies. Only a perfect match is used to estimate the intensity of probe set. Cross-hybridization is accounted for in model estimation. Remarkable reproducibility between replicate samples has been attained at our Gene Microarray Core Facility (21). Zhang *et al.* (21) recommend using as criteria for differential expression between two chips a $|\log_2 \text{ratio}| > 0.8$ and mean $\log_2$ signal >7.9. The contrasts were limited to comparison between treated *versus* untreated samples in each cell line. Subsequently, a comparison of gene expression was made between methods and cell lines. The results of contrasts with Affymetrix software include the following: 1) detection p values; 2) log ratios with 95% confidence intervals; and 3) change p values (one-sided). The p values are from one-sided tests of up-regulation in expression. The results of contrasts with Zhang's Perfect Match software include the following: 1) mean Log_2 signal and 2) $\log_2$ ratio. The results for the four contrasts described above were exported to Excel spreadsheets. Although log ratio >0.8 produced some consistency, we have used log ratio >1.0, corresponding to a 2-fold change, as the final selection criteria for the differentially expressed genes in this study.

Reverse Transcription-PCR Analysis—To verify the analysis results (Table I) from Affymetrix chip hybridization, total RNA was reverse-transcribed with a random hexamer or T7-$(dT)_{24}$ primer (Invitrogen). An aliquot (50 ng of total RNA) of the first strand cDNA was used as a template for PCR. Two genes (*DEEPEST* and *H4FG* listed in Table I) that lacked the validated primer sets and probes for real time PCR were examined in this study with regular RT-PCR. Oligonucleotide sequences of the primer sets used in this study are as follows: mitotic spindle coiled-coil protein (*DEEPEST*), sense (S)-AGCTGGAACAGGACCTAGCA and antisense (AS)-TCTGGGTAAGCTGGCAGAGT; H4 histone family, member G (*H4FG*), S-TAAGGTGCTCCGGGATAACA and AS-CCCTGACGTTTTAGGGCATA; and glyceraldehyde phosphate dehydrogenase (*GAPDH*), S-GAGTCAACGGATTTGGTCGT and AS-TTGATTTTGGAGGGATCTCG. To monitor better the amplification efficiency and to control experimental errors, a duplex PCR that simultaneously amplified two genes, one internal control *GAPDH* and one gene of interest (*DEEPEST* or *H4FG*) in the same tube, was adopted. Duplex PCR was carried out in 50 μl containing 50 ng of cDNA, 50 pmol of each primer (25 pmol for *H4FG* primer set), 20 mM $(NH4)_2SO_4$, 75 mM Tris-HCl (pH 8.8), 1.5 mM $MgCl_2$, 0.01% (v/v) Tween 20, and 0.2 mM each of dATP, dCTP, dGTP, and dTTP, using 1.25 units of Taq polymerase (Invitrogen). The following conditions were used: 95 °C, 3 min followed by 25 (*H4FG*) or 35 (*DEEPEST*) cycles of denaturation (95 °C, 30 s), annealing (59 °C (*DEEPEST*) or 62 °C (*H4FG*), 30 s), and extension (72 °C (*DEEPEST*) or 68 °C (*H4FG*), 45 s). The reaction was incubated at 72 °C for 10 min at the conclusion of the PCR cycle. The resulting PCR product was analyzed by ethidium bromide-agarose gel electrophoresis. Bands were subjected to densitometric analysis and were normalized to expression of the internal control *GAPDH*. All validation experiments using duplex PCR were performed by two independent technicians and confirmed in both SKBr3 and BT474 cell lines. Two end cycle numbers were used for *DEEPEST* (35 (better) and 40) and *H4FG* (25 (better) and 30). To exclude any possible contamination or errors, a positive control and a negative control were included in each experiment.

Quantitative Real Time RT-PCR Analysis—To validate gene expression changes, quantitative real time RT-PCR analysis was performed with an Applied Biosystems Prism 7900HT Sequence Detection System using TaqMan® universal PCR master mix according to the manufacturer's specifications (Applied Biosystems Inc., Foster City, CA) for the 14 genes listed in Table I for which validated TaqMan Gene Expression Assays are available. The TaqMan probes and primers for *CKS2* (assay identification number Hs00829071_s1), *HEC* (assay identification number Hs00196101_m1), *MAD3L* (assay identification number Hs00176169_m1), *STK15* (assay identification number Hs00269212_m1), *UBE2C* (assay identification number Hs00853610_g1), *ZWINT* (assay identification number Hs00199952_m1), *FEN1* (assay identification number Hs00748727_s1), *PCNA* (assay identification number Hs00427214_g1), *RFC4* (assay identification number Hs00427469_m1), *TOP2A* (assay identification number Hs00172214_m1), *TYMS* (assay identification number Hs00426591_m1), *HMG2* (assay identification number Hs00357789_g1), *KIAA186* (assay identification number Hs00221421_m1), and *PHLDA2* (assay identification number Hs00169368_m1) were assay-on-demand gene expression products (Applied Biosystems). Human *GAPDH* gene was used as endogenous control (Applied Biosystems, catalog number 4326317E). The gene-specific probes were labeled by using reporter dye FAM, and the *GAPDH* internal control probe was labeled with a different reporter dye VIC at the 5′ end. A nonfluorescent quencher and the minor groove binder were linked at the 3′ end of probe as quenchers. The thermal cycler conditions were as follows: hold for 10 min at 95 °C, followed by two-step PCR for 40 cycles of 95 °C for 15 s followed by 60 °C for 1 min. All samples were performed in triplicate. Amplification data were analyzed with an Applied Biosystems Prism Sequence Detection Software version 2.1 (Applied Biosystems). To normalize the relative expression of the genes of interest to the *GAPDH* control, standard curves were prepared for each gene mentioned above and the *GAPDH* in each experiment. When the efficiency of the target gene amplification and the efficiency of *GAPDH* amplification were approximately equal, which was proven by examining the absolute value (less than 0.1) of the slope of log input amount *versus* ΔC_T, the $\Delta\Delta C_T$ method recommended by the manufacturer was used to compare the relative expression levels between treatments. When the efficiency of the target gene amplification and the efficiency of *GAPDH* amplification were not equal, the relative expression model of Pfaffl (see Ref. 19), which considered the effect of different efficiencies between samples, was used to calculate the relative expression levels of samples.

Preparation of Total Cell Lysate, Immunoprecipitation, and Immunoblot Analysis—These procedures were performed as described previously (16).

Immunohistochemical Staining—The method was basically performed as described previously (22). Briefly, 4D5- or trastuzumab-treated cells were deposited on glass slides using Cytospin 3 (Thermo Electron Corp., Waltham, MA). The slides were air-dried and fixed with 4% paraformaldehyde at room temperature for 30 min. Slides were then washed in PBS and incubated with 3% H_2O_2 in methanol for 30 min to eliminate endogenous peroxidase activity. Nonspecific binding of primary antibodies was blocked by incubation with 5% skim milk for 30 min, and slides were then incubated with the PCNA monoclonal antibody (dilution of 1:2000) at room temperature for 2 h. The slides were then washed three times with PBS, incubated for 30 min at room temperature with 1:30 diluted biotinylated anti-immunoglobulins link (BioGenex, San Ramon, CA), and followed by incubation in label reagent (BioGenex) for 30 min at room temperature. After applying the substrate solution (BioGenex), the slides were washed thoroughly with distilled water and mounted with aqueous mounting oil.

Generation of Dominant Positive AKT1 Construct and Stable Transfection—The human full-length *AKT1* sequence coupled with an N-

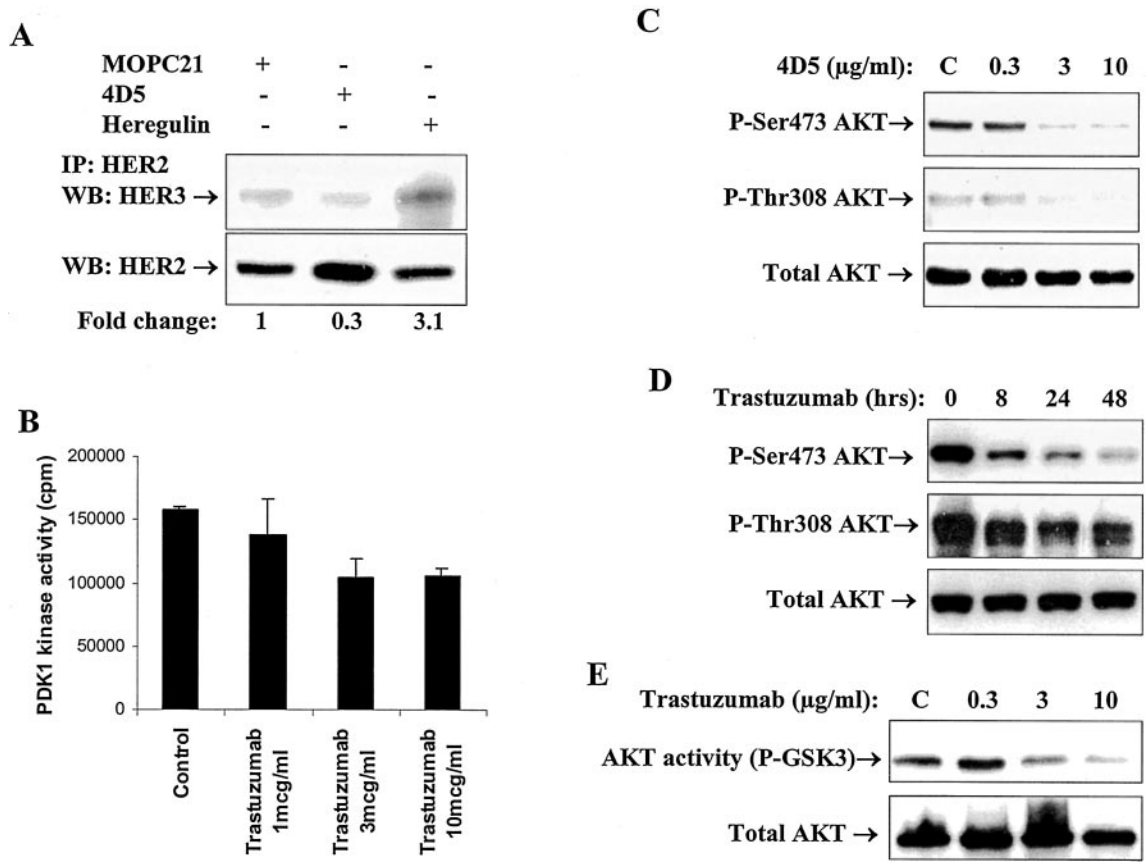

FIG. 1. **Anti-HER2 antibody decreased PI3K-AKT signaling activity.** *A*, 4D5 decreased HER2-HER3 interaction. SKBr3 cells were treated with 4D5 (10 μg/ml), MOPC21 (10 μg/ml), or heregulin (30 ng/ml) for 24 h and subjected to immunoprecipitation using anti-HER2 antibody ID5 as described under "Materials and Methods." Immunoprecipitates (*IP*) were analyzed by Western blotting (*WB*) with an anti-HER3 antibody. The blot was stripped and reprobed with anti-c-Neu antibody. The *numbers below* the gel figure show the relative expression of HER3, which was obtained by densitometry after normalization with HER2 expression. *B*, anti-HER2 antibody trastuzumab inhibited PDK1 activity. BT474 cells were treated with trastuzumab at different concentrations or control hIgG (10 μg/ml) for 48 h and subjected to PDK1 assay as described under "Materials and Methods." *C*, 4D5 decreased both serine and threonine phosphorylation of AKT at 473 and 308 sites in SKBr3 cells. SKBr3 cells were treated with 4D5 at different concentrations or control antibody (MOPC21 at 10 μg/ml) for 24 h and subjected to total protein extraction and Western blotting. The blot was probed with two phospho-AKT antibodies. The blot was then stripped and reprobed with anti-total AKT antibody. *C* indicates control antibody MOPC21. *D*, trastuzumab decreased both Ser-473 and Thr-308 phosphorylation of AKT in BT474 cells. BT474 cells were treated with trastuzumab (10 μg/ml) for different intervals and subjected to total protein extraction and Western blotting. The blot was probed with two phospho-AKT antibodies. The blot was then stripped and reprobed with anti-total AKT antibody. *E*, trastuzumab inhibited AKT activity. BT474 cells were treated with trastuzumab at different concentrations or control hIgG (10 μg/ml) for 48 h and subjected to an AKT assay as described under "Materials and Methods." *C* indicates control antibody hIgG. All experiments in this figure were at least repeated three times and showed similar results.

terminal myristoylation sequence (*mAKT1*) was obtained by RT-PCR using the primer set (left primer sequence, 5′-CAGCCTGAGAGGAGCGCGTGAGCGTCG-3′; right primer sequence, 5′-GCTATCGTCCAGCGCAGTCCAC-3′) and total RNA from OVCAR3 cells. The amplified *mAKT1* fragment was then cloned into pCRTOPO2.1 vector (Invitrogen). The activated *AKT1* construct was then subcloned into pcDNA3.0 expression vector (Invitrogen). The human *AKT1* and myristoylation sequences in pcDNA3.0 vector were confirmed by DNA sequencing. SKBr3 cells were transfected with the appropriate expression plasmids (*mAKT1* or empty vector pcDNA3.0) by using Lipofectamine-2000 (Invitrogen) as recommended by the manufacturer.

Anchorage-dependent Cell Growth Assay—A crystal violet cell growth assay in a 96-well microplate was used to assess the anchorage-dependent growth as described previously (26).

Cell Cycle Analysis—The method was performed as described previously (6).

Statistical Analysis—The two-tailed Student's *t* test was used to compare different groups. Values with $p < 0.05$ were considered significant.

RESULTS

Anti-HER2 Antibody Significantly Inhibits PI3K-AKT Signaling—In a previous report (16), we demonstrated that treatment with anti-HER2 antibody decreased PI3K activity and reduced phosphorylation of AKT on Ser-473 (Ser-473 AKT). In this report, we have extended these studies to determine the mechanisms by which anti-HER2 antibody mediates these actions by investigating the effect of anti-HER2 antibody on HER2-HER3 association, phosphoinositide-dependent kinase-1 (PDK1) kinase activity, phosphorylation of AKT at threonine 308 (Thr-308 AKT), and AKT enzymatic activity. As demonstrated previously (23, 24), the signaling from HER2 to PI3K-AKT pathway depends on the formation of HER2-HER3 heterodimers because HER3 has multiple consensus binding sites for the p85 PI3K subunit. To measure association of HER2 and HER3, complexes were immunoprecipitated with the ID5 anti-HER2 antibody (6), and Western blots were probed with anti-HER2 and anti-HER3 antibodies. Treatment of SKBr3 cells with 4D5 decreased the association of HER2 and HER3 by 70% when compared with MOPC21 control, whereas the association was enhanced by 3.1-fold under treatment with the ligand heregulin (Fig. 1*A*). PDK1 kinase, which is recruited to the membrane by the PtdIns products of PI3K, is an immediate downstream target of PI3K and is responsible for the phosphorylation of Thr-308 on AKT (25). The PDK1 enzymatic activity was inhibited by trastuzumab in a concentration-dependent manner (Fig. 1*B*). Consistent with our previous observations (16), phosphorylation of Ser-473 AKT was down-regulated by 4D5 or trastuzumab treatment in both SKBr3

TABLE I
Differential expression of genes that are induced by anti-HER2 antibody

Gene name	Gene symbol	Fold change[a]		Function
		SKBr3	BT474	
Pleckstrin homology-like domain, family A	*PHLDA2*	−2.42	−2.44	Fas expression
KIAA0186 gene product	*KIAA186*	−2.93	−2.67	Unknown
CDC28 protein kinase 2	*CKS2*	−2.01	−2.72	Cell cycle
High mobility group protein 2	*HMG2*	−2.46	−2.73	Chromatin
Mitotic spindle coiled-coil related protein	*DEEPEST*	−2.21	−3.00	Cell cycle, spindle
Topoisomerase (DNA) II α	*TOP2A*	−2.01	−3.01	DNA replication
Ubiquitin-conjugating enzyme E2C	*UBE2C*	−2.05	−3.36	Cell cycle, mitosis
Flap structure-specific endonuclease 1	*FEN1*	−2.18	−3.36	DNA repair and synthesis
Proliferating cell nuclear antigen	*PCNA*	−2.02	−3.41	DNA replication and repair
Replication factor C (activator 1) 4	*RFC4*	−2.01	−3.46	DNA replication and repair
Mitotic checkpoint kinase Mad3L	*MAD3L*	−2.24	−3.57	Cell cycle, mitosis
Thymidylate synthetase	*TYMS*	−2.21	−3.77	DNA replication
ZW10 interactant	*ZWINT*	−2.32	−3.92	Cell cycle, spindle
Serine/threonine kinase 15	*STK15*	−2.42	−4.28	Cell cycle, spindle
Highly expressed in cancer	*HEC*	−2.56	−4.72	Cell cycle, spindle
H4 histone family, member G	*H4FG*	−2.60	−4.88	Chromatin

[a] Fold change represents expression ratio of anti-HER2 antibody-treated sample over control antibody-treated sample in average sample.

and BT474 cells (Fig. 1, *C* and *D*). As shown in Fig. 1, *C* and *D*, phosphorylation of Thr-308 AKT was also down-regulated by 4D5 or trastuzumab treatment in concentration- and time-dependent manners in both SKBr3 and BT474 cell lines. Enzymatic activity of AKT was also significantly inhibited by trastuzumab in a concentration-dependent manner (Fig. 1*E*). Thus, anti-HER2 antibodies significantly inhibited cellular signaling through the PI3K-AKT pathway.

Treatment with Anti-HER2 Antibody Down-regulates Genes That Participate in Regulation of the Cell Cycle, Cell Growth, Cell Maintenance, and Chromatin Structure—To elucidate the mechanism by which inhibition of PI3K signaling contributes to the effects of anti-HER2 antibody, we have evaluated the impact of anti-HER2 antibody and of direct PI3K inhibition on gene expression by SKBr3 and BT474 breast cancer cells that overexpress HER2. Cells were treated with anti-HER2 antibody (4D5 or trastuzumab) or control antibody (MOPC21 or hIgG). Total RNA was isolated to permit synthesis of cRNA for Affymetrix array hybridization. The U95Av2 gene chip was used to measure expression of 12,000 known human genes. Every hybridized chip underwent quality control checks as described under "Materials and Methods." Based on the two methods of array analysis describe above, anti-HER2 antibody down-regulated expression of 30 genes in SKBr3 and 123 genes in BT474. Treatment with anti-HER2 antibody up-regulated expression of 19 genes in SKBr3 and 16 genes in BT474 cells. When changes in both cell lines were considered, 24 genes were down-regulated and 4 genes were up-regulated. Attempts to validate these differences, however, suggested that more stringent criteria would be required to eliminate false positives. When genes were selected that exhibited a log ratio >1.0, corresponding to a 2-fold change in both cell lines, 16 genes were down-regulated, and no genes were up-regulated (Table I). RT-PCR, real time PCR, Western blotting, or immunohistochemistry subsequently confirmed the differential expression of all 16 genes. Thus, anti-HER2 antibody exerted a predominantly inhibitory effect on gene expression in breast cancer cells that overexpressed HER2.

Among the 16 differentially expressed genes, 15 had previously been identified, and one gene (*KIAA0186*) had not been characterized. Of the 15 known genes, 14 fell into three functional areas as follows: cell cycle regulation, DNA repair/replication, and chromatin structure (Table I). With the aid of Affymetrix functional annotation software, we have compared the fraction of differentially expressed genes in each of 20 functional categories relative to the fraction in each category for all of the genes on the Hu95Av2 chip. Of the 16 antibody-regulated genes, 64% had roles in cell growth/maintenance and 52% contributed to cell cycle progression. On the U95Av2 chip, only 5 and 35% of genes belonged to cell growth/maintenance and to the cell cycle, respectively. The data suggest that the genes involved in cell cycle and cell growth/maintenance were preferentially regulated by anti-HER2 antibody.

Anti-HER2 Antibody Preferentially Down-regulates Genes That Participate in the G_2-M Phase of the Cell Cycle—Seven genes (*STK15, CKS2, DEEPEST, UBE2C, MAD3L, ZWINT*, and *HEC*) that relate to cell cycle control were down-regulated by 2.0–4.7-fold by anti-HER2 antibody (Table I). One notable feature of these seven cell cycle genes is that all participate in the G_2-M phase, especially spindle formation, which could relate to the synergistic anti-tumor activity observed between taxanes and anti-HER2 antibody. To confirm these seven cell cycle genes were down-regulated by anti-HER2 antibody treatment, real time RT-PCR (six genes) and duplex RT-PCR (*DEEPEST*) were performed as described under "Materials and Methods." SKBr3 cells were treated with 4D5 or MOPC21 control antibody for 24 h before extraction of total RNA. As shown in Fig. 2*A*, six genes were down-regulated by anti-HER2 antibody treatment in a concentration-dependent manner as detected by real time PCR. Consistent with the Affymetrix array data, all six genes were down-regulated 35–80% at the highest concentration of 4D5 in SKBr3 cells (Fig. 2*A*). To validate further these gene expression changes, BT474 cells were treated with trastuzumab or control hIgG antibody for 48 h before isolation of total RNA. Similar to the 4D5-treated SKBr3 cells, concentration-dependent inhibition of all six genes was confirmed by real time PCR in trastuzumab-treated BT474 cells (Fig. 2*B*). The level of *DEEPEST* expression was also shown by duplex PCR to decrease after trastuzumab treatment in BT474 cells (Fig. 2, *C* and *D*). *DEEPEST* expression was also inhibited by 4D5 treatment in SKBr3 cells (data not shown). The availability of a specific antibody permitted further confirmation of the down-regulation of the STK15 protein level by Western blot analysis as shown in Fig. 2*E*. Thus, anti-HER2 antibody significantly down-regulates cell cycle genes that particularly impact on the cell cycle G_2-M transition.

Anti-HER2 Antibody Down-regulates Genes Involved in Control of DNA Repair and Replication—Five genes (*PCNA, TOP2A, RFC4, TYMS*, and *FEN1*) involved in control of DNA repair and replication were down-regulated 2.0–3.8-fold by anti-HER2 antibody (Table I). PCNA down-regulation was not only confirmed by real time RT-PCR (Fig. 3*A*) but also confirmed at protein level by Western blotting (Fig. 3*B*) and im-

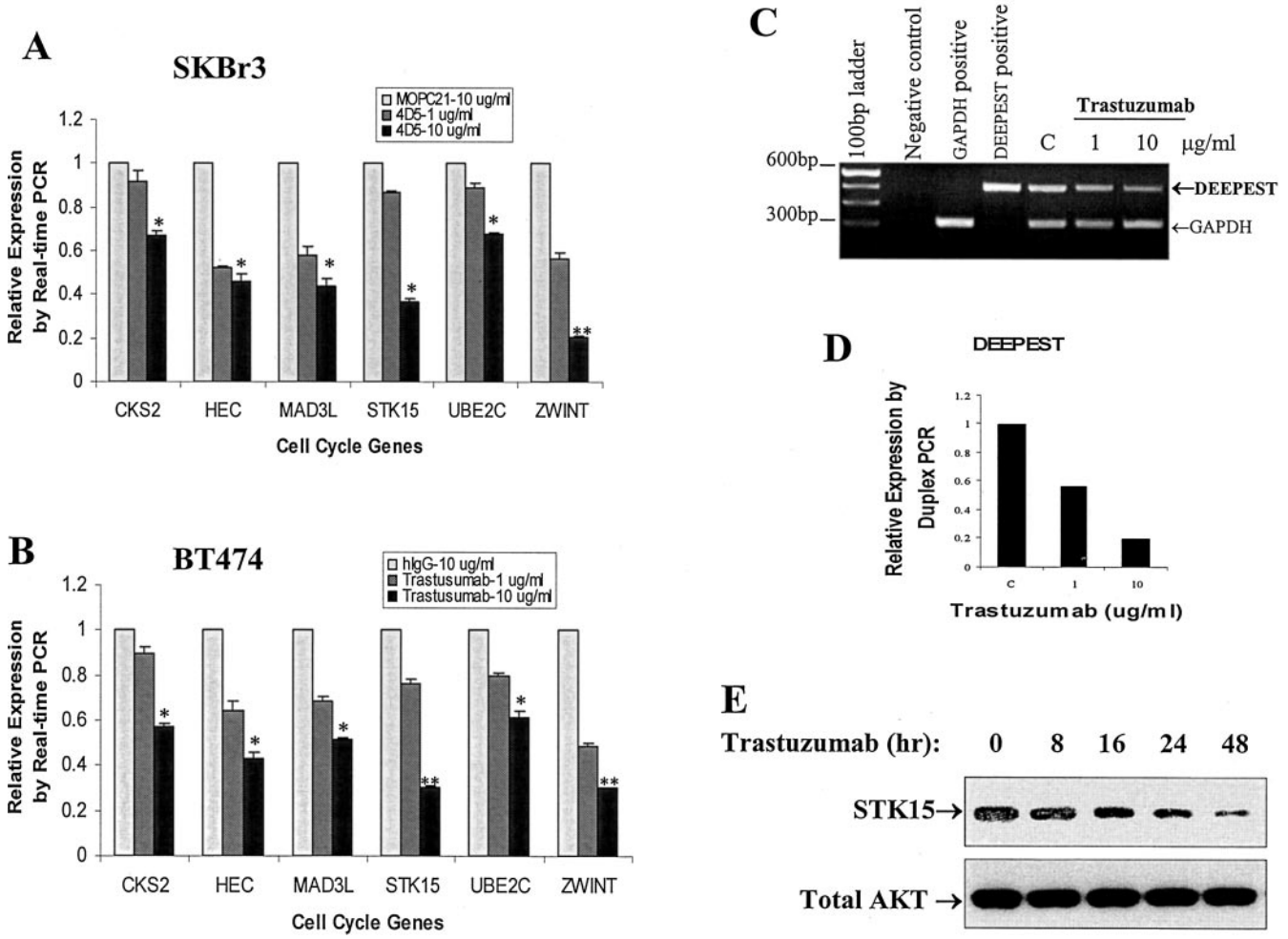

FIG. 2. **Validation of cell cycle-related genes.** The seven cell cycle-related genes, *CKS2*, *DEEPEST*, *HEC*, *STK15*, *MAD3L*, *UBE2C*, and *ZWINT*, were assessed by real time RT-PCR or duplex RT-PCR analysis as described under "Materials and Methods" in both SKBr3 cells and BT474 cells. *A*, real time RT-PCR analysis of six cell cycle genes in SKBr3 cells. * depicts results statistically significantly different relative to the control group ($p < 0.05$). ** depicts results statistically significantly different relative to the control group ($p < 0.01$). *B*, real time RT-PCR analysis of six cell cycle genes in BT474 cells. *C*, duplex RT-PCR analysis of *DEEPEST* gene expression in BT474 cells treated with trastuzumab. A representative ethidium bromide-stained agarose gel picture is shown. The RT-PCR results were repeated three times. *C* indicates control antibody hIgG (10 μg/ml). *D*, normalization of *DEEPEST* expression with the internal reference *GAPDH* expression as shown in *C*. *E*, anti-HER2 antibody decreases the level of STK15 protein. BT474 cells were treated with trastuzumab at 10 μg/ml for different intervals and harvested for total protein extraction. Western blotting was performed to check STK15 expression with a rabbit anti-STK15 antibody.

munohistochemical staining (Fig. 3*C*) in both SKBr3 and BT474 cell lines. The decrease in *PCNA* RNA level was more dramatic in trastuzumab-treated BT474 cells than that in 4D5-treated SKBr3 cells (Fig. 3*A*). The decrease in expression of PCNA protein was more significant than that of *PCNA* RNA in SKBr3 cells (Fig. 3*B*). The other anti-HER2 regulated genes that participate in DNA repair and replication control, *RFC4, TOP2A, TYMS,* and *FEN1*, were also confirmed by real time RT-PCR in both SKBr3 cells (Fig. 4*A*) and BT474 cells (Fig. 4*B*). Down-regulation of *RFC4*, *TOP2A*, *TYMS*, and *FEN1* expression by the antibodies was concentration-dependent (Fig. 4). *FEN1*, *RFC4*, and *TOP2A* were all down-regulated by more than 50% by the antibody treatment. The magnitude of down-regulation of *TYMS* was relatively modest, whereas inhibition of TOP2A expression was more prominent (Fig. 4). Thus, anti-HER2 antibody is able to negatively affect genes involved in DNA replication and repair.

Anti-HER2 Antibody Down-regulates Genes That Modify Chromatin Structure—The two genes *H4FG* and *HMG2* that regulate chromatin structure and gene transcription were down-regulated 2.5–4.9-fold by the anti-HER2 antibody. Duplex RT-PCR (for *H4FG* shown in Fig. 5, *A–C*) and real time RT-PCR (for *HMG2* shown in Fig. 5, *D* and *E*) confirmed the concentration-dependent down-regulation of these two chromatin-associated genes in both SKBr3 (Fig. 5, *A*, *B* and *D*) and BT474 (Fig. 5, *C* and *E*) cell lines treated with the anti-HER2 antibodies. These results revealed, for the first time, that chromatin-associated genes are one of the targets of the anti-HER2 antibody.

Direct PI3K Inhibition Down-regulates Genes That Are Also Decreased by the Anti-HER2 Antibody—Treatment with anti-HER2 antibody inhibits cancer cell growth, blocks signaling through PI3K-AKT, and down-regulates genes that control cell cycle, DNA repair/replication, and modify chromatin structure. To test the hypothesis that at least some genes down-regulated by treatment with anti-HER2 antibody are regulated by PI3K signaling, breast cancer cells that overexpress HER2 were treated with chemical inhibitors of PI3K to determine whether or not the genes down-regulated by the antibody are down-regulated by direct inhibition of PI3K. Real time RT-PCR and duplex RT-PCR (for *DEEPEST* and *H4FG*) were performed to assess the effects of PI3K inhibition. As shown in Fig. 6*A*, inhibition of PI3K with LY294002 suppressed expression of six cell cycle-related genes (*CKS2, HEC, MAD3L, STK15, UBE2C,* and *ZWINT*) in a concentration-dependent manner as demonstrated by real time PCR, resembling the activity of the anti-

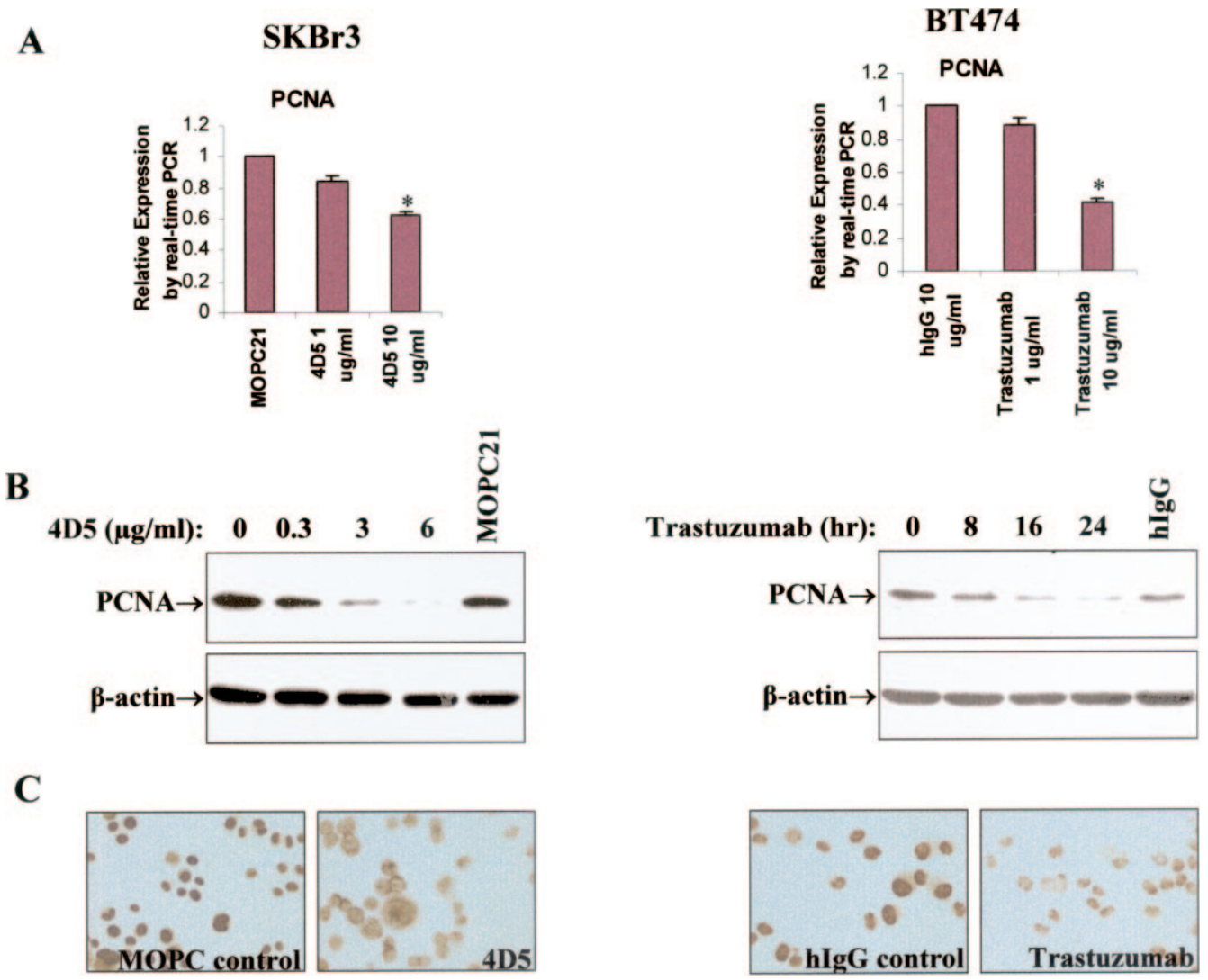

FIG. 3. **Validation of PCNA expression.** *A*, *PCNA* expression was detected by real time RT-PCR as described under "Materials and Methods" in SKBr3 cells and in BT474 cells. * depicts results statistically significantly different relative to the control group ($p < 0.05$). *B*, PCNA level was detected by Western blotting. SKBr3 cells were treated with control antibody MOPC21 (6 μg/ml) or anti-HER2 antibody 4D5 at different concentrations (24-h incubation). BT474 cells were treated with control antibody hIgG (10 μg/ml) or anti-HER2 antibody trastuzumab (10 μg/ml) at different time intervals. Cells were then harvested for total protein extraction. Western blotting was performed to check PCNA expression using a monoclonal anti-PCNA antibody. This result was repeated three times. *C*, cells were treated with trastuzumab (BT474 for 48 h) or 4D5 (SKBr3 for 24 h) at 10 μg/ml and spun onto slides by cytospin. Immunohistochemistry staining was performed using a monoclonal anti-PCNA antibody as described under "Materials and Methods." The *brown* staining in the nucleus is the PCNA signal. This result was repeated three times.

HER2 antibody shown in Fig. 2. Results from duplex RT-PCR indicated another cell cycle-related gene *DEEPEST* was also dose-dependently inhibited by LY294002 treatment (Fig. 6*B*). Five DNA replication and repair-related genes (*FEN1, PCNA, RFC4, TOP2A,* and *TYMS*) were suppressed by LY294002 treatment as detected by real time PCR (Fig. 6*C*). LY294002 treatment also significantly reduced the expression of two chromatin structure-related genes *HMG2* and *H4FG* as demonstrated by real time PCR (Fig. 6*D*) and duplex PCR (Fig. 6*E*), respectively. These data suggest that LY294002 and anti-HER2 antibody exert similar effects to some magnitude on the above-mentioned 14 differentially expressed genes, consistent with the possibility that PI3K signaling mediates some of the transcriptional effects of anti-HER2 antibody.

Constitutive Activation of AKT1 Blocks the Ability of Anti-HER2 Antibody to Down-regulate Genes and to Induce Cell Cycle G_1 Arrest—If signaling through the PI3K pathways, particularly the PI3K-AKT pathway, mediates down-regulation of the relevant genes, then expression of a dominant positive AKT might blunt the response to anti-HER2 antibodies. Consequently, we constructed a mammalian expression vector for dominant positive AKT1 (mAKT1) and stably transfected it into SKBr3 cells. As shown in Fig. 7*A*, the established mAKT1 clone expressed a high level of AKT1 protein that was functionally active as illustrated by strong phosphorylation of both Ser-473 and Thr-308. The effects of anti-HER2 antibody on the differentially expressed genes and cell cycle were tested in two active mAKT1 clones. The expression of active mAKT1 blocked the down-regulation of *CKS2*, *HEC, UBE2C,* and *ZWINT* genes (cell cycle-related, Fig. 7*B*); of *RFC4* and *TYMS* genes (DNA replication and repair-related, Fig. 7*B*); and of *HMG2* and *H4FG* genes (chromatin-related, Fig. 7, *B* and *C*) induced by the anti-HER2 antibody. Most interestingly, active mAKT1 did not block the down-regulation of *DEEPEST, MAD3L, STK15* (cell cycle-related, Fig. 7, *D* and *E*), *FEN1, PCNA*, and *TOP2A* (DNA replication/repair related, Fig. 7*E*) by the anti-HER2 antibody. Anti-HER2 antibody did down-regulate the expression of these 14 genes in the control clones that contained the empty vector pcDNA 3.0 (data not shown). As expected, expression of active mAKT1 (Fig. 7*F*) stimulated the cell cycle pro-

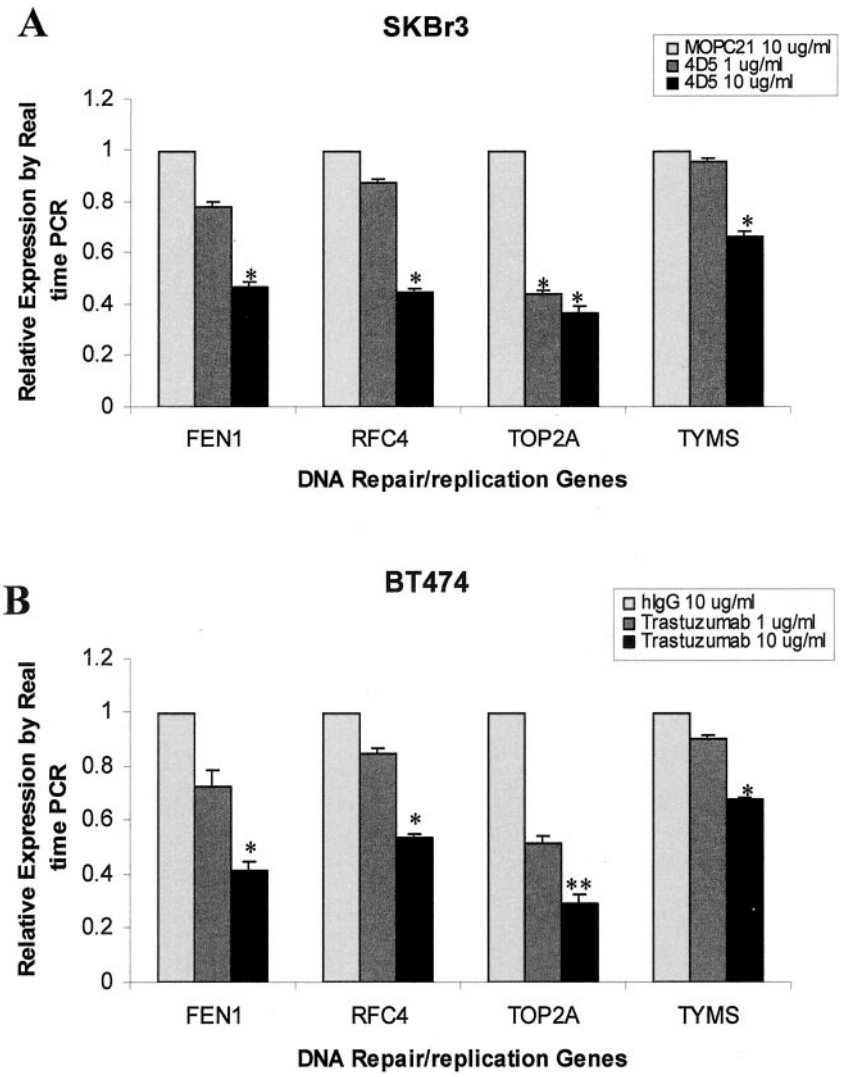

FIG. 4. **Validation of DNA repair and replication-related genes.** The four DNA repair and replication-related genes *RFC4*, *TOP2A*, *TYMS*, and *FEN1* were assessed by real time RT-PCR as described under "Materials and Methods" in SKBr3 cells (*A*) and in BT474 cells (*B*). * depicts results statistically significantly different relative to the control group ($p < 0.05$). ** depicts results statistically significantly different relative to the control group ($p < 0.01$).

gression evidenced by fewer cells in the G_1 phase (36.2–45.1%) when compared with the control clone (61.9%). Expression of active mAKT1 decreased 4D5-mediated G_1 accumulation from control 78 to 41.4 or to 51% in the two clones (Fig. 7*F*), indicating mAKT1 severely impaired anti-HER2 antibody-induced cell cycle G_1 arrest. Taken together, these data demonstrate that the differentially expressed genes were, at least in part, regulated by PI3K-AKT signaling, and inhibition of the PI3K-AKT pathway is an important mechanism for the activity of anti-HER2 antibody.

Anti-HER2 Antibody Enhances Docetaxel-induced Growth Inhibition Associated with Enhanced Down-regulation of HEC and DEEPEST Expression—Anti-HER2 antibody was shown to enhance the toxicity of paclitaxel in pre-clinical and clinical settings (3, 26). Taxane derivatives, including paclitaxel and docetaxel, are anti-mitotic agents that target microtubules and thus spindle function and arrest cell cycling in G_2-M (27). Treatment of breast cancer cells with anti-HER2 antibodies reduced expression of the genes that particularly regulate spindle in the G_2-M phase of the cell cycle (Fig. 2 and Table I). These data prompted us to investigate the effects of combined treatment with anti-HER2 antibody and docetaxel on these seven cell cycle genes identified in this study. Inhibition of anchorage-dependent cell growth of SKBr3 cells with a combination of 4D5 anti-HER2 antibody and docetaxel was confirmed using a crystal violet mitogenic assay (12, 26). As shown in Fig. 8*A*, 4 nM docetaxel inhibited SKBr3 cell growth by 62.5%, whereas anti-HER2 antibody 4D5 (5 μg/ml) alone inhibited growth by 51%. A combination of 4D5 and docetaxel produced significantly greater inhibition of 81%, whereas control antibody and docetaxel produced 60% growth inhibition (Fig. 8*A*). Most surprisingly, the combination of 4D5 and docetaxel did not induce more apoptotic cells (25.6%) than did MOPC and docetaxel (30.4%) (Fig. 8*B*). Compared with the control group MOPC21 plus docetaxel, more cells accumulated in the G_1 phase and fewer cells in the G_2-M phase in combination treatment with 4D5 and docetaxel (Fig. 8*B*). These results suggested that the effect of anti-HER2 antibody on cell cycle regulation might contribute to its ability to potentiate the growth inhibition of docetaxel. When the expression of cell cycle-related genes was assayed, a combination of 4D5 antibody and docetaxel additively down-regulated the expression level of *HEC* (by real time PCR) and *DEEPEST* (by duplex PCR), whereas docetaxel alone and control antibody plus docetaxel did not alter or slightly increased the expression of *HEC* and *DEEPEST* (Fig. 8, *C* and *D*). The other five cell cycle genes that were regulated by anti-HER2 antibody (*CKS2, STK15, UBE2C, MAD3L,* and *ZWINT*) were not further down-regulated by treatment with a combination of 4D5 and docetaxel (data not shown). Thus, enhanced down-regulation of *HEC* and *DEEPEST* expression by anti-HER2 antibody and docetaxel was associated with greater inhibition of tumor growth in breast cancer cells that overexpress HER2.

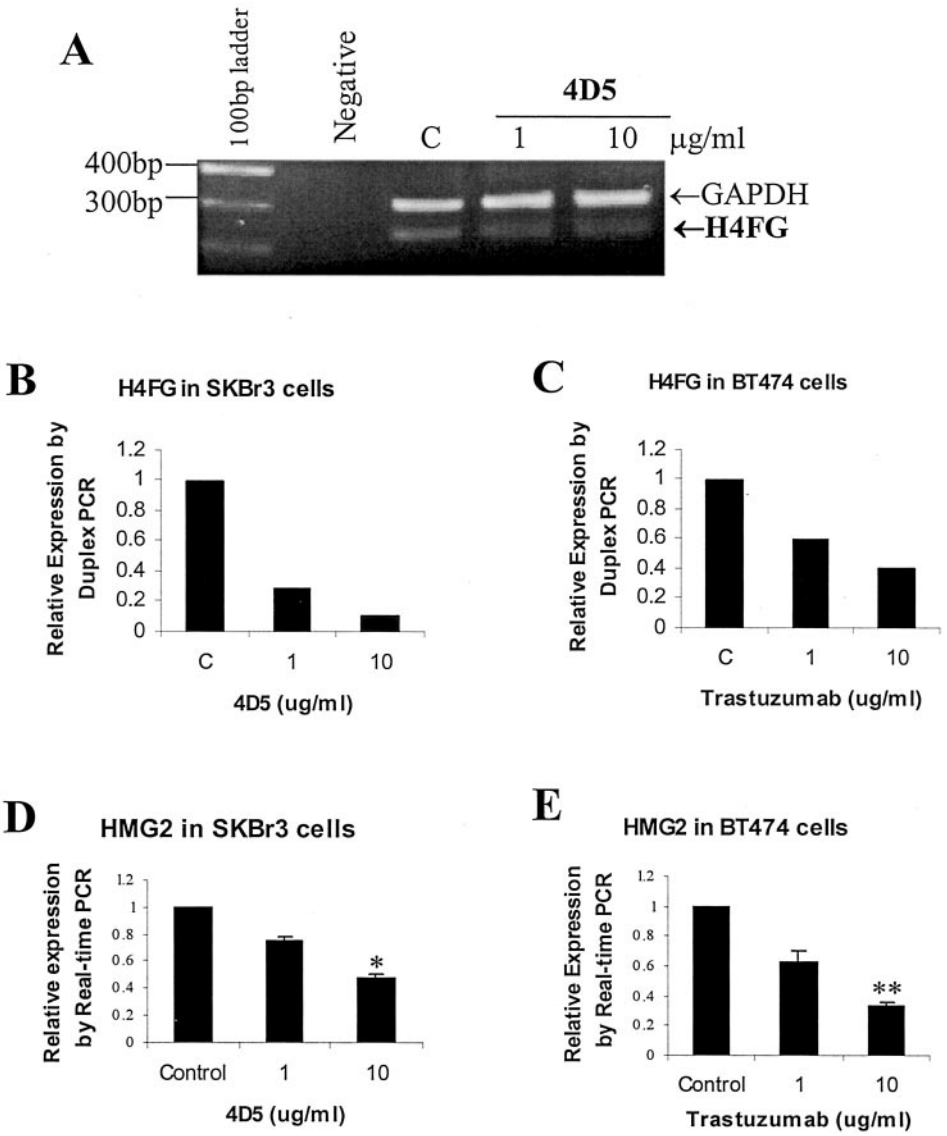

FIG. 5. **Validation of chromatin-associated genes.** The two chromatin-associated genes were assessed by duplex RT-PCR (*H4FG*) and real time RT-PCR (*HMG2*) analysis as described under "Materials and Methods" in SKBr3 cells and in BT474 cells. *A*, *H4FG* and *GAPDH* expression were revealed by duplex PCR in SKBr3 cells. A representative ethidium bromide-stained agarose gel picture was shown. This duplex PCR experiment was repeated three times with similar results. *C* in the panel indicates control antibody MOPC21 (10 μg/ml). *B*, normalization of *H4FG* expression level with internal control *GAPDH* expression as shown in *A* in SKBr3 cells. *C*, semi-quantitative level of *H4FG* expression in BT474 cells under the same conditions stated in *A* and *B*. *D*, real time RT-PCR analysis of *HMG2* gene expression in SKBr3 cells. * depicts results statistically significantly different relative to the control group ($p < 0.05$). *E*, real time RT-PCR analysis of *HMG2* gene expression in BT474 cells. ** depicts results statistically significantly different relative to the control group ($p < 0.01$).

DISCUSSION

Treatment of breast cancer cells that overexpress HER-2 with anti-HER2 antibody inhibited HER2-HER3 association, decreased PDK1 activity, reduced Thr-308 and Ser-473 phosphorylation of AKT, and reduced AKT enzymatic activity. Decreased signaling through AKT could result from interference with the formation of HER2-HER3 heterodimers, preventing phosphorylation of HER3 and docking of PI3K subunits. Crystal structure was recently resolved at 2.5 Å for the entire extracellular domain of HER2 complexed with trastuzumab (38). Trastuzumab binds to domain IV of the receptor on the C-terminal portion of the juxtamembrane region of HER2 at a site containing the binding pocket for an extended domain II loop that mediates formation of inter-receptor dimers (38). Thus, anti-HER2 antibodies 4D5 and trastuzumab could block the HER2-HER3 interaction, thus preventing activation of the PI3K-AKT pathway. Data in Fig. 1 support this possibility and confirm previous observations that anti-HER2 antibodies inhibit PI3K-AKT signaling (11, 16, 17).

To define the possible mechanism(s) of action of anti-HER2 antibody, gene expression in breast cancer cells treated with anti-HER2 antibody was compared with that in cells treated with control antibody. Sixteen genes were significantly down-regulated by anti-HER2 antibody, 15 with known function and 1 not yet characterized. Fourteen of the 15 known genes were classified into the following three major functional areas: 7 in cell cycle regulation largely related to the G_2-M phase; 5 in DNA repair/replication; and 2 affecting chromatin structure (Table I). Anti-HER2 antibody had the greatest impact on genes affecting cell cycle and cell growth/maintenance (Table I). One pro-apoptotic gene (*PHLDA2*) was down-regulated by anti-HER2 antibody. PHLDA2 may enhance Fas expression (28), but decreased expression after treatment with anti-HER2 antibody suggests that transcriptional regulation of this gene does not contribute to antibody-mediated growth inhibition.

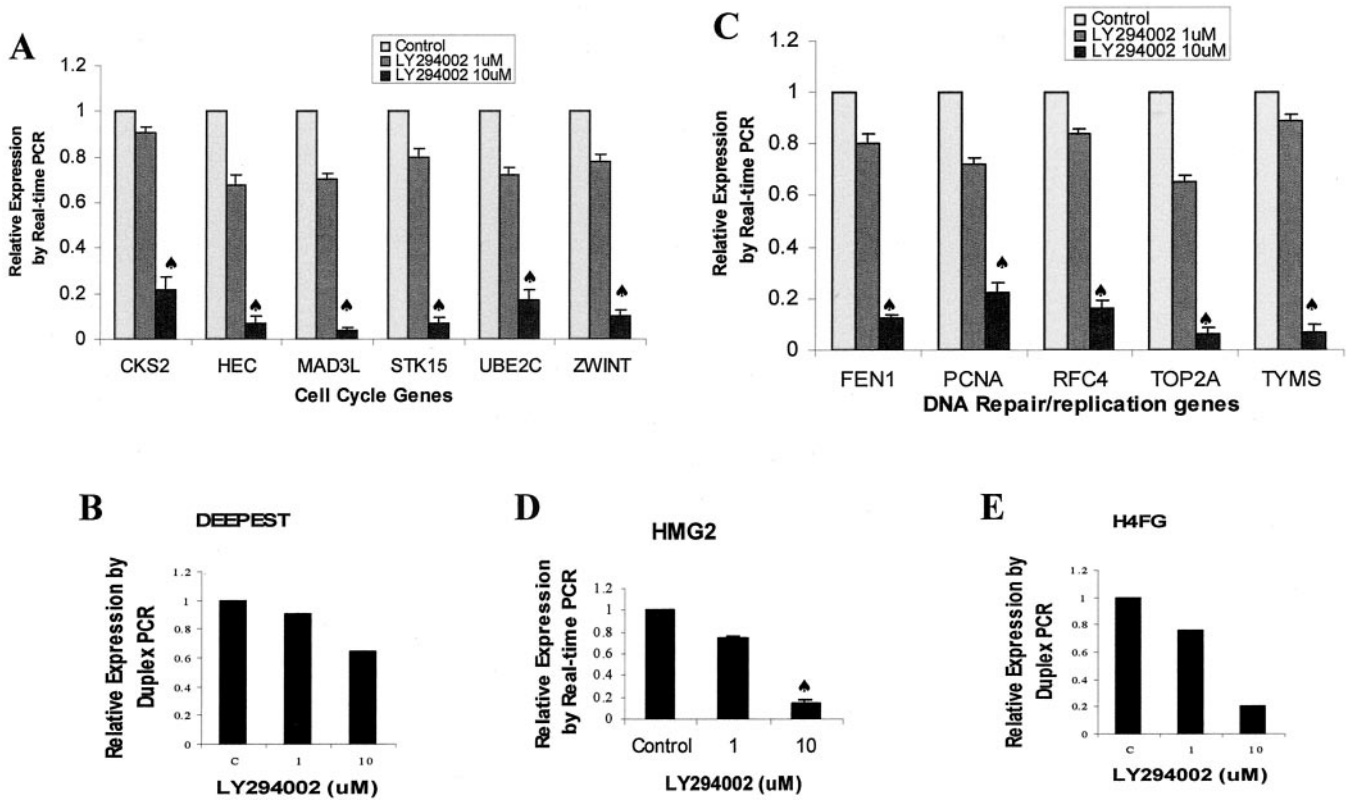

FIG. 6. **Direct inhibition of PI3K with LY294002 mimicked the effects of anti-HER2 antibody on the expression of differentially expressed genes.** SKBr3 cells were treated with diluent (Me_2SO) or LY294002 at different concentrations for 24 h and subjected to total RNA extraction and real time RT-PCR and duplex RT-PCR analysis. *A*, real time RT-PCR analysis of expression of six cell cycle-related genes. ♠ depicts results statistically significantly different relative to the control group ($p < 0.01$). *B*, expression of the *DEEPEST* gene revealed by duplex PCR. This duplex PCR experiment was repeated three times with similar results. *C* in the panel indicates the Me_2SO control. Shown was the relative expression of *DEEPEST* after normalization with the internal *GAPDH* expression. *C*, real time RT-PCR analysis of expression of five DNA replication and repair-related genes. ♠ depicts results statistically significantly different relative to the control group ($p < 0.01$). *D*, real time RT-PCR analysis of *HMG2* gene expression. ♠ depicts results statistically significantly different relative to the control group ($p < 0.01$). *E*, duplex RT-PCR analysis of *H4FG* gene expression. *C* in the panel means the Me_2SO control. Shown is the relative expression of *H4FG* gene after normalization with the internal *GAPDH* expression.

A combination of trastuzumab and paclitaxel additively inhibits growth of human breast cancer cell lines (26). Treatment of mice bearing human breast cancer xenografts using a combination of trastuzumab and paclitaxel rendered 59% of animals tumor free, compared with 17.3% of mice treated with paclitaxel alone (29). Clinical studies have demonstrated substantially greater benefit when trastuzumab and paclitaxel are used concurrently to treat patients with metastatic breast cancers that overexpress HER2 (30). The mechanisms underlying the interaction between paclitaxel and trastuzumab remain unclear. Recently, sensitization of paclitaxel-induced apoptosis by anti-HER2 antibody has been proposed as an important mechanism underlying additive growth inhibition (20). The combination of docetaxel and trastuzumab has also been shown to be active against breast cancers that overexpress HER2 (31). Most surprisingly, treatment with anti-HER2 antibody did not enhance docetaxel-induced apoptosis. Rather, the addition of anti-HER2 antibody increased growth inhibition without a further increase in the fraction of apoptotic cells. Enhanced growth inhibition was associated with enhanced down-regulation of two genes involved in the G_2-M phase of the cell cycle, *HEC* and *DEEPEST* (Fig. 8). Although trastuzumab may increase paclitaxel-induced apoptosis in some cell lines (20), we believe that inhibition of expression of cell cycle G_2-M genes by anti-HER2 antibody also may contribute to the molecular mechanisms by which anti-HER2 antibody enhances the anti-tumor activity of docetaxel.

Trastuzumab can also suppress DNA repair capacity (18), possibly contributing to the enhancement of the anti-tumor effect of cisplatin and of radiotherapy. Among the DNA repair/replication genes, *TOP2A*, a key enzyme in DNA replication, is located adjacent to the *HER2* oncogene at the chromosome location 17q12-q21 and is either amplified or deleted in almost 90% of HER2-amplified primary breast tumors (32). TOP2A expression was down-regulated by anti-HER2 antibody on Affymetrix arrays, and decreased gene expression was confirmed in both cell lines by real time PCR (Fig. 4). By decreasing TOP2A activity, treatment with anti-HER2 antibody might also enhance the chemosensitivity to topoisomerase II-inhibitors such as etoposide. Recently, Liang *et al.* (41) have reported that trastuzumab induces radiosensitization of breast cancer cell lines that overexpress HER2 through the PI3K-AKT pathway. Our data in Figs. 3, 4, and 7 demonstrated that trastuzumab down-regulated five genes that related to DNA repair/replication control (*FEN1, PCNA, RFC4, TOP2A,* and *TYMS*) through the PI3K pathways. Therefore, this study suggests one mechanism by which trastuzumab can potentiate the efficacy of radiotherapy and DNA-damaging agents on breast cancer cells that overexpress HER2.

The negative effect of anti-HER2 antibody on genes associated with regulation of chromatin structure is a novel observation that suggests additional mechanisms of action for anti-HER2 antibody. Both H4FG and HMG2 are chromatin-associated proteins that are able to bend DNA into DNA circles and to facilitate cooperative interactions between cis-acting

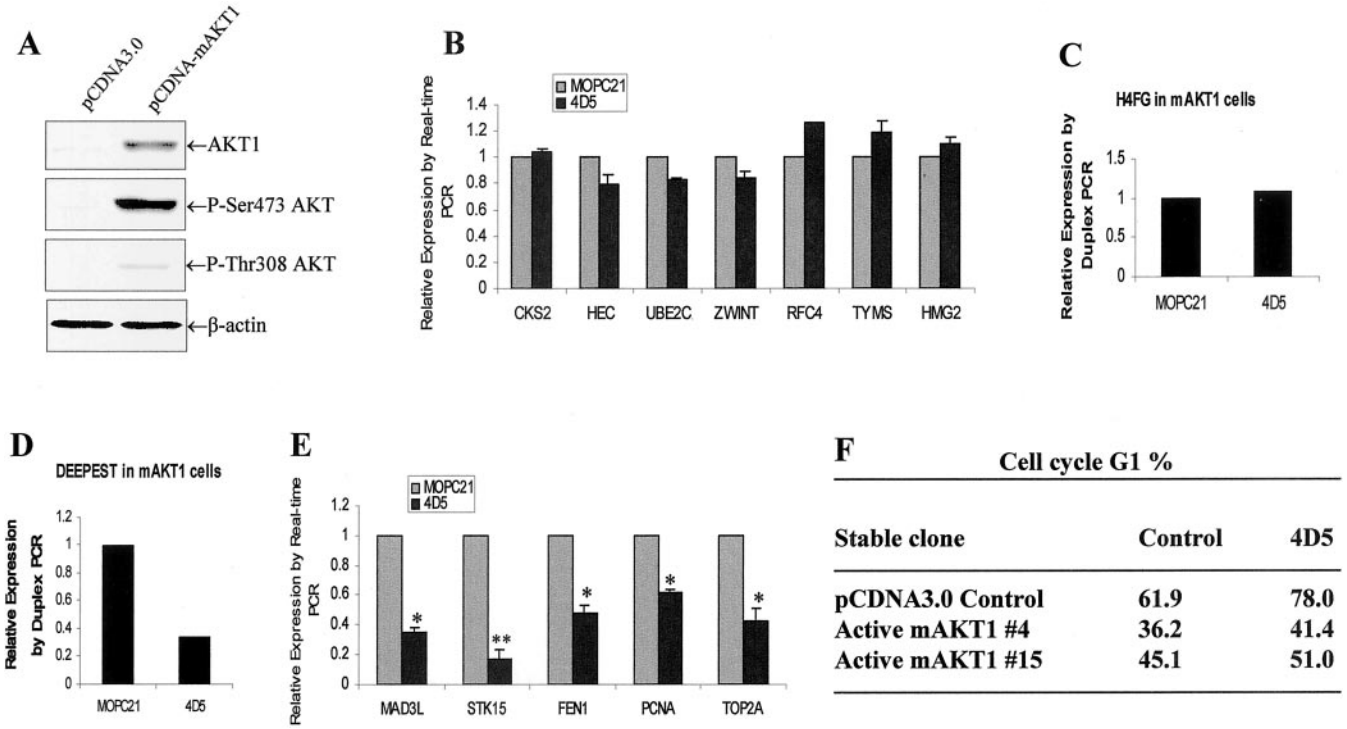

Stable clone	Control	4D5
pCDNA3.0 Control	61.9	78.0
Active mAKT1 #4	36.2	41.4
Active mAKT1 #15	45.1	51.0

FIG. 7. **Constitutive activation of AKT1 blocks the effect of anti-HER2 antibody on differentially expressed genes and on cell cycle arrest.** *A*, establishment of constitutively active AKT1 clones in SKBr3 cells. SKBr3 cells were transfected with a mAKT1 construct and stable clones that overexpressed AKT1 were selected as described under "Materials and Methods." An example of one stable mAKT1 clone is shown. *B*, real time RT-PCR analysis of expression of *CKS2*, *HEC*, *UBE2C*, *ZWINT*, *RFC4*, *TYMS*, and *HMG2* genes. Cells from mAKT1 clone 4 were treated with 4D5 or control antibody MOPC21 at 10 μg/ml for 24 h. Total RNA extraction, cDNA preparation, and real time RT-PCR analysis were performed as described under "Materials and Methods." *C*, duplex RT-PCR analysis of the *H4FG* gene in mAKT1 cells. Cells were treated as described in *B*. This duplex PCR experiment was repeated three times with similar results. Shown is the relative expression of the *H4FG* gene after normalization with the internal *GAPDH* expression. *D*, duplex RT-PCR analysis of *DEEPEST* gene in mAKT1 cells. Cells were treated as described in *B*. This duplex PCR experiment was repeated three times with similar results. Shown is the relative expression of *DEEPEST* gene after normalization with the internal *GAPDH* expression. *E*, real time RT-PCR analysis of expression of *MAD3L*, *STK15*, *FEN1*, *PCNA*, and *TOP2A* genes. Experimental procedures were performed at same conditions as described in *B*. *F*, mAKT1 clones 4 and 15 were treated with 4D5 (10 μg/ml) or control antibody MOPC21 (10 μg/ml) for 24 h and harvested for cell cycle analysis as described under "Materials and Methods." Shown is a representative of two similar results.

proteins (33, 34). Cis-acting proteins, in turn, facilitate modification of chromatin. HER2-overexpressing breast cancer cells contain significantly higher levels of acetylated and phosphorylated histone H3 and acetylated histone H4 associated with the HER2 promoter (35). Inhibitors of histone deacetylase such as trichostatin A and sodium butyrate can down-regulate transcription of HER2 (36). A 33-kDa kinase associated with chromatin structure can be phosphorylated as a consequence of HER2 signaling (37). Therefore, it is possible that anti-HER2 antibody could regulate target gene expression and activity through modification of histone acetylation/phosphorylation.

The ability of anti-HER2 antibody and inhibition of PI3K to down-regulate a coordinate set of genes suggests that anti-HER2 antibody mediates its effects, at least in part, through inhibition of signaling through the PI3K-AKT pathway. This contention is supported by the observation that activated AKT can largely bypass the effects of anti-HER2 antibody on the expression of a number of genes. Although the PI3K-AKT pathway is most commonly associated with G_1/S progression and cell survival, a number of recent publications have implicated the PI3K-AKT signaling cascade in regulation of the G_2-M checkpoints as well (38–40). Our studies, which demonstrated that PI3K inhibitor down-regulates the expression of seven G_2-M phase genes (*CKS2, DEEPEST, MAD3L, HEC, STK15, UBE2C,* and *ZWINT*), support the role of PI3K-AKT in the G_2-M phase. These results suggest that the PI3K-AKT pathways may be involved in a greater number of cellular functions than hypothesized previously.

Expression of active mAKT1 blocked anti-HER2 antibody-induced inhibition of eight genes but did not block expression of the other six genes (Fig. 7). This interesting observation suggests that the PI3K-AKT1 pathway is not the only signaling pathway involved in regulation of the cell cycle and DNA replication/repair. Two chromatin structure-related genes, *H4FG* and *HMG2*, may be primarily regulated through the PI3K-AKT pathway, based on the results shown in Fig. 7, *B* and *C*. Other AKT isoforms and/or PI3K pathways such as PI3K-SGK3, PI3K-p70S6K, PI3K-PTEN, PI3K-Raf, and others may also be involved in the regulation of these genes and in the mechanisms of action for the antibody. We suggest[2] that trastuzumab has a negative effect on SGK3 and p70S6K activities as well. Because the mAKT1 cells were resistant to treatment with anti-HER2 antibody (Fig. 7*F*), we believe that PI3K-AKT is a critical pathway but not the only pathway that mediates the mechanisms of action for the antibody.

As we have shown previously, anti-HER2 antibody blocks HER2-overexpressed breast cancer cells at the G_1 phase of the cell cycle and reduces the number of cells at the S phase (6, 12). This work illustrates that anti-HER2 antibody markedly down-regulates the expression of seven G_2-M phase genes (*STK15*, *CKS2*, *DEEPEST*, *UBE2C*, *MAD3L*, *ZWINT*, and *HEC*). We believe that this down-regulation of the G_2-M phase genes could result from cell cycle G_1 arrest. In consideration of the new role of PI3K-AKT in cell cycle G_2-M phase, it is also

[2] X.-F. Le and R. C. Bast, Jr., unpublished data.

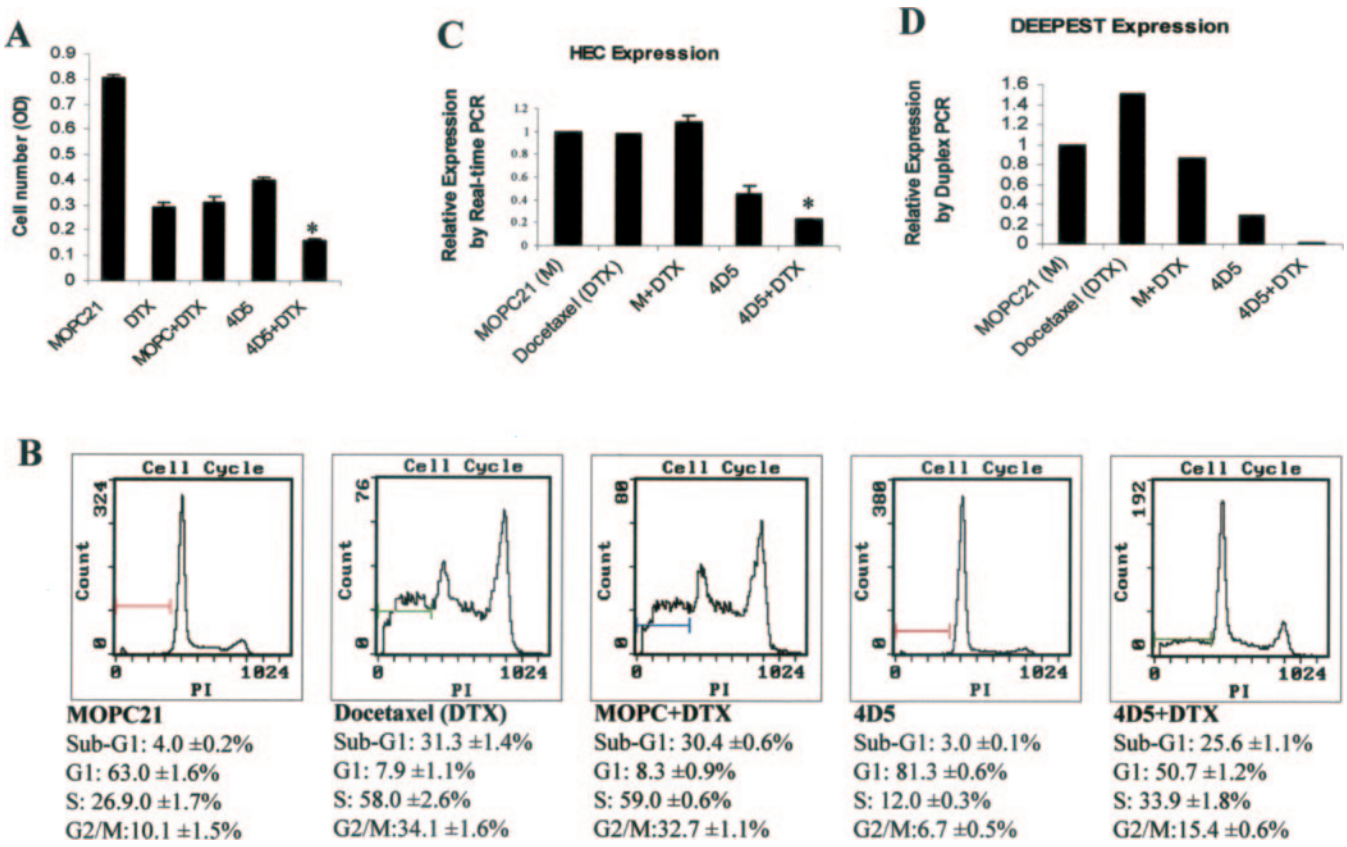

FIG. 8. **Potentiation of docetaxel-induced growth inhibition by anti-HER2 antibody is associated with additive down-regulation of *HEC* and *DEEPEST* gene expression**. *A*, anti-HER2 antibody enhances docetaxel-induced growth inhibition. The anchorage-dependent growth assay was carried out in 96-well microplates as stated under "Materials and Methods." SKBr3 cells were treated with antibodies (MOPC21 or 4D5) and docetaxel (*DTX*) simultaneously or individual agent alone for 3 days. * indicates results statistically significantly different relative to the control group ($p = 0.02$). *B*, 4D5 plus docetaxel combination do not produce higher apoptosis but more cells in the cell cycle G_1 phase. SKBr3 cells were treated as stated in *A* and harvested for cell cycle analysis as described under "Materials and Methods." Shown is a representative of five results. *C*, 4D5 plus docetaxel combination is associated with additive down-regulation of *HEC* gene expression. SKBr3 cells were treated as stated in *A* and subjected to total RNA isolation and real time RT-PCR analysis. * depicts results statistically significantly different relative to the control group ($p < 0.05$). *D*, 4D5 plus docetaxel combination is associated with additive down-regulation of *DEEPEST* gene expression. Cells were treated as stated in *A* and subjected to total RNA isolation and duplex RT-PCR analysis. Shown is the relative expression of *DEEPEST* gene after normalization with the internal *GAPDH* expression. This experiment was repeated three times with similar results.

possible that anti-HER2 antibody may have dual impact on both G_1 and G_2-M checkpoints, which leads to arrest and disruption of regular cell cycle and thus to inhibition of proliferation of HER2-overexpressed breast cancer cells.

The data presented here provides new evidence related to the pathways by which anti-HER2 antibody inhibits proliferation and acts in concert with docetaxel to decrease tumor growth. Anti-HER2 antibody primarily affects the genes involved in cell cycle progression, particularly in the G_2-M phase, DNA repair and replication, and chromatin modification. Our results further demonstrated that inhibition of PI3K-AKT signaling is an important mechanism by which the anti-HER2 antibody induces cell cycle G_1 arrest and down-regulates a number of target genes. These data show that the potentiation of growth inhibition with the combination of anti-HER2 antibody and docetaxel is associated with enhanced down-regulation of two G_2-M phase genes, *HEC* and *DEEPEST*.

Acknowledgments—We sincerely thank Deepa Deshpande for performing the PDK1 assay and Dr. Michael Frumovitz and Andrea Patterson for helpful discussions regarding Affymetrix array analysis. Affymetrix GeneChip hybridization and imaging data analysis were performed at the M. D. Anderson Genomics Facility, which is supported in part by the Cancer Center Support Grant CA16672. We also thank Karen Ramirez at the Flow Cytometry Core Laboratory (South Campus, also supported by CA16672) for expert assistance with flow cytometric analysis.

REFERENCES

1. Citri, A., Skaria, K. B., and Yarden, Y. (2003) *Exp. Cell Res.* **284,** 54–65
2. Stern, D. F. (2003) *Exp. Cell Res.* **284,** 89–98
3. Pegram, M. D., Konecny, G., Slamon, D. J. (2000) *Cancer Treat. Res.* **103,** 57–75
4. Holbro, T., Civenni, G., and Hynes, N. E. (2003) *Exp. Cell Res.* **284,** 99–110
5. Arteaga, C. L. (2003) *Breast Cancer Res.* **5,** 96–100
6. Le, X.-F., McWatters, A., Wiener, J., Mills, G. B., and Bast, R. C., Jr. (2000) *Clin. Cancer Res.* **6,** 260–270
7. Neve, R. M., Sutterluty, H., Pullen, N., Lane, H. A., Daly, J. M., Krek, W., and Hynes, N. E. (2000) *Oncogene* **19,** 1647–5166
8. Pietras, R. J., Poen, J. C., Gallardo, D., Wongvipat, P. N., Lee, H. J., and Slamon, D. J. (1999) *Cancer Res.* **59,** 1347–1355
9. Sliwkowski, M. X., Lofgren, J. A., Lewis, G. D., Hotaling, T. E., Fendly, B. M., and Fox, J. A. (1999) *Semin. Oncol.* **26,** Suppl. 12, 60–70
10. Lane, H. A., Beuvink, I., Motoyama, A. B., Daly, J. M., Neve, R. M., and Hynes, N. E. (2000) *Mol. Cell. Biol.* **20,** 3210–3223
11. Yakes, F. M., Chinratanalab, W., Ritter, C. A., King, W., Seelig, S., and Arteaga, C. L. (2002) *Cancer Res.* **62,** 4132–4141
12. Le, X.-F., Claret, F. X., Lammayot, A., Tian, L., Deshpande, D., LaPushin, R., Tari, A. M., and Bast, R. C., Jr. (2003) *J. Biol. Chem.* **278,** 3441–3450
13. Baselga, J., Albanell, J., Molina, M. A., and Arribas, J. (2001) *Semin. Oncol.* **28,** Suppl. 16, 4–11
14. Kono, K., Takahashi, A., Ichihara, F., Sugai, H., Fujii, H., and Matsumoto, Y. (2002) *Cancer Res.* **62,** 5813–5817
15. Clynes, R. A., Towers, T. L., Presta, L. G., and Ravetch, J. V. (2000) *Nat. Med.* **6,** 443–446
16. Le, X.-F., Vadlamudi, R., McWatters, A., Bae, D. S., Mills, G. B., Kumar, R., and Bast, R. C., Jr. (2000) *Cancer Res.* **60,** 3522–3531
17. Hermanto, U., Zong, C. S., and Wang, L. H. (2001) *Oncogene* **20,** 7551–7562
18. Pietras, R. J., Pegram, M. D., Finn, R. S., Maneval, D. A., and Slamon, D. J. (1998) *Oncogene* **17,** 2235–2249
19. Pfaffl, M. W. (2001) *Nucleic Acids Res.* **29,** 2002–2007
20. Lee, S., Yang, W., Lan, K. H., Sellappan, S., Klos, K., Hortobagyi, G., Hung, M. C., and Yu, D. (2002) *Cancer Res.* **62,** 5703–5710

21. Zhang, L., Miles, M. F., and Aldape, K. D. (2003) *Nat. Biotechnol.* **21,** 818–821
22. Le, X.-F., Vallian, S., Mu, Z. M., Hung, M. C., and Chang, K. S. (1998) *Oncogene* **16,** 1839–1849
23. Prigent, S. A., and Gullick, W. J. (1994) *EMBO J.* **13,** 2831–2841
24. Holbro, T., Beerli, R. R., Maurer, F., Koziczak, M., Barbas, C. F., III, and Hynes, N. E. (2003) *Proc. Natl. Acad. Sci. U. S. A.* **100,** 8933–8938
25. Vanhaesebroeck, B., and Alessi, D. R. (2000) *Biochem. J.* **346,** 561–576
26. Pegram, M. D., Finn, R. S., Arzoo, K., Beryt, M., Pietras, R. J., and Slamon, D. J. (1997) *Oncogene* **15,** 537–547
27. Orr, G. A., Verdier-Pinard, P., McDaid, H., and Horwitz, S. B. (2003) *Oncogene* **22,** 7280–7295
28. Qian, N., Frank, D., O'Keefe, D., Dao, D., Zhao, L., Yuan, L., Wang, Q., Keating, M., Walsh, C., and Tycko, B. (1997) *Hum. Mol. Genet.* **6,** 2021–2029
29. Baselga, J., Norton, L., Albanell, J., Kim, Y. M., and Mendelsohn, J. (1998) *Cancer Res.* **58,** 2825–2831
30. Slamon, D. J., Leyland-Jones, B., Shak, S., Fuchs, H., Paton, V., Bajamonde, A., Fleming, T., Eiermann, W., Wolter, J., Pegram, M., Baselga, J., and Norton, L. (2001) *N. Engl. J. Med.* **344,** 783–792
31. Esteva, F. J., Valero, V., Booser, D., Guerra, L. T., Murray, J. L., Pusztai, L., Cristofanilli, M., Arun, B., Esmaeli, B., Fritsche, H. A., Sneige, N., Smith, T. L., and Hortobagyi, G. N. (2002) *J. Clin. Oncol.* **20,** 1800–1808
32. Jarvinen, T. A., Tanner, M., Barlund, M., Borg, A., and Isola, J. (1999) *Genes Chromosomes Cancer* **26,** 142–150
33. Paull, T. T., Haykinson, M. J., and Johnson, R. C. (1993) *Genes Dev.* **7,** 1521–1534
34. Marzluff, W. F., Gongidi, P., Woods, K. R., Jin, J., and Maltais, L. J. (2002) *Genomics* **80,** 487–498
35. Mishra, S. K., Mandal, M., Mazumdar, A., and Kumar, R. (2001) *FEBS Lett.* **507,** 88–94
36. Scott, G. K., Marden, C., Xu, F., Kirk, L., and Benz, C. C. (2002) *Mol. Cancer Ther.* **1,** 385–392
37. Samanta, A., and Greene, M. I. (1995) *Proc. Natl. Acad. Sci. U. S. A.* **92,** 6582–6586
38. Kandel, E. S., Skeen, J., Majewski, N., Di Cristofano, A., Pandolfi, P. P., Feliciano, C. S., Gartel, A., and Hay, N. (2002) *Mol. Cell. Biol.* **22,** 7831–7841
39. Shtivelman, E., Sussman, J., and Stokoe, D. (2002) *Curr. Biol.* **12,** 919–924
40. Tran, H., Brunet, A., Grenier, J. M., Datta, S. R., Fornace, A. J., Jr., DiStefano, P. S., Chiang, L. W., and Greenberg, M. E. (2002) *Science* **296,** 530–534
41. Liang, K., Lu, Y., Jin, W., Ang, K. K., Milas, L., and Fan, Z. (2003) *Mol. Cancer Ther.* **2,** 1113–2110